PHYSICAL REVIEW B **66**, 024207 (2002)

Microscopic and macroscopic parameters of energy transfer between Tm^{3+} ions in fluoroindogallate glasses

D. F. de Sousa and L. A. O. Nunes

Instituto de Física de São Carlos, Universidade de São Paulo, Caixa Postal 369 CEP 13560-970, São Carlos, SP, Brazil

(Received 13 November 2001; revised manuscript received 30 April 2002; published 26 July 2002)

In this work a rate equations formalism is used to study the kinetics of the $^3H_4$ and $^3F_4$ levels of Tm^{3+} ions in fluoroindogallate glasses. Emphasis is given to the determination of the microscopic and macroscopic parameters of the energy transfer processes $^3H_4, ^3H_6 \rightarrow ^3F_4, ^3F_4$ and $^3H_4, ^3H_6 \rightarrow ^3H_6, ^3H_4$. The 1/*e* time of the $^3H_4$ level in function of Tm^{3+} concentration was simulated by using the macroscopic energy transfer rates obtained with the microparameters of energy transfer up to the quadrupole-quadrupole order of interaction. It was found that the quadrupole-quadrupole coupling dominates the mentioned energy transfer processes in such way that a reduction of about 22% in the estimation of the $^3F_4$ level steady state population is observed if only the dipole-dipole coupling is taken into account.

DOI: 10.1103/PhysRevB.66.024207 PACS number(s): 78.20.−e, 78.55.−m

I. INTRODUCTION

Energy transfer between rare-earth ions has been a topic of interest in the study of solid-state lasers. Particularly, the optical properties of Tm^{3+} ions have been studied in a variety of crystalline hosts, solutions, and glass matrices.[1] The Tm^{3+} based laser at approximately 1800 nm ($^3F_4 \rightarrow ^3H_6$ electronic transition) is attractive for medical and lidar applications.[2,3] In addition, the Tm^{3+} has a strong absorption band around 800 nm which matches the AlGaAs semiconductor lasers wavelength. In order to achieve an optimized solid state device at 1800 nm it is necessary to know in detail the fluorescence properties of the Tm^{3+} ion in the host material. Characteristics such as emission cross-section and pumping efficiency are crucial to determine the feasibility of the laser system.

It is well known that the pumping mechanism of the $^3F_4$ level is the cross-relaxation $^3H_4, ^3H_6 \rightarrow ^3F_4, ^3F_4$ (ion 1, ion 2→ion 1, ion 2) which results in two Tm^{3+} ions excited at the upper laser level by one pump photon. The energy migration $^3H_4, ^3H_6 \rightarrow ^3H_6, ^3H_4$ enhances the cross-relaxation probability as it spreads the excitation energy into the host material. In this sense, these energy transfer probabilities and efficiencies are features directly related to the pump efficiency. The energy transfer processes occurs between rare-earth ions mediated mainly by multipolar interactions. It is a common practice to attribute the dipole-dipole type interaction to treat the energy transfer among impurities diluted in a solid medium. Most of the papers that have studied the mentioned Tm^{3+}:Tm^{3+} interactions consider only the dipole-dipole coupling to describe the energy transfer.[4–8] However, high-order-energy transfer mechanisms, such as dipole-quadrupole or quadrupole-quadrupole may be important in rare-earth doped samples if the electronic transitions involved in the energy transfer processes are electric quadrupole permitted and the interagent ions are close enough.[9–14] This is so because as the electric dipole transitions are parity forbidden in rare-earth ions, the electric quadrupole transitions can compete with electric dipole ones in the energy transfer. Tonooka and co-workers[15] estimated the contribution of the higher-order interactions in the $Tb^{3+} \rightarrow Nd^{3+}$ energy transfer by means of Monte Carlo simulation. It was found that the dipole-quadrupole interaction is the best one to describe the decay curves of the Tb^{3+} $^1D_2$ level. Tkachuck[13,16] have studied the higher order interactions in Tm^{3+} doped yttrium lithium fluoride (YLF) crystals and concluded that the macroscopic rates must include the dipole-quadrupole and quadrupole-quadrupole interactions in order to fully describe the $^3H_4$ decay.

In a recent paper[17] the energy transfer microparameters for the processes $^3H_4, ^3H_6 \rightarrow ^3F_4, ^3F_4$ and $^3H_4, ^3H_6 \rightarrow ^3H_6, ^3H_4$ for dipole-dipole, dipole-quadrupole, and quadrupole-quadrupole coupling were calculated by means of the Dexter[18] and Kushida[19] models. In this work, a rate equations formalism is used to describe the kinetic behavior of the $^3H_4$ and $^3F_4$ levels. The already obtained microparameters are used to determine the average macroparameters of energy transfer that are related to the rate equations. The proceedings outlined here were previously used to treat upconversion photoluminescence between Nd^{3+} ions in ZBLAN glasses, YLF and YAG crystals, and also Cr^{3+} interactions in LiSrCaF.[20–23] In these previous works the dipole-dipole coupling was the only active mechanism of energy transfer. On the other hand, for Tm:Tm interactions we have to obtain the expressions for the macroparameters in the high-order multipole couplings.

II. EXPERIMENTAL SETUP

The used set of samples has the following nominal molar composition: $30PbF_2$-$15InF_3$-$20GaF_3$-$15ZnF_2$-$(20\text{-}X)CaF_2$-$XTmF_3$, with $X = 0.1$, 0.5, 1.0, 2.0, 4.0, 6.0, and 7.0, henceforth named *X*Tm. The Tm^{3+} concentrations were measured by energy dispersive x-ray analysis with a digital microscope and the Link Analytical QX2000 software. The measured concentrations range from $(1.2 \pm 0.8) \times 10^{20}$ up to $(15.0 \pm 0.8) \times 10^{20}$ cm^{-3}. The refractive index of the samples for the Sodium D line is 1.570. Optical absorption experiments in the ultraviolet-visible-near infrared range

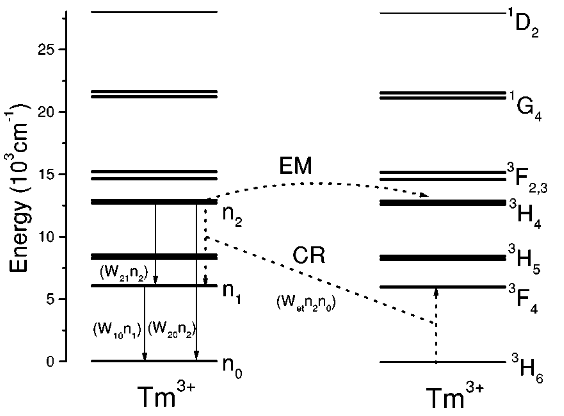

FIG. 1. (a) Energy levels diagram of the Tm^{3+} ions in fluoroindogallate glasses.

were done using a Perkin-Elmer Lambda 900 spectrophotometer. Photoluminescence in the near infrared range (from 800 to 2000 nm) was performed using a Ti:sapphire laser operating at 778 nm to excite the Tm^{3+} ions to the $^3H_4$ level. This wavelength was chosen to permit a resonant measurement of the luminescent signal. After being dispersed by a 0.25 m Czerny-Turner monochromator, the signal was detected by an InAs photodetector, amplified by a Lock-in, and recorded by the computer. For the lifetime measurements of the $^3H_4$ and $^3F_4$ levels, the pump source was a homemade dye laser (dye LDS 698) at 680 nm pumped by a Nd:YAG laser at 532 nm. The signal was acquired by a photomultiplier tube RCA 31034 (for the 800 nm signal) or an InAs detector (for the 2000 nm signal) and recorded at a digital oscilloscope Tektronix TDS 380.

III. RESULTS

Figure 1 shows the energy levels diagram obtained from the absorption spectra of the Tm^{3+} in fluoroindogallate glasses. The cross relaxation (CR) ($^3H_4,^3H_6 \rightarrow ^3F_4,^3F_4$) and the energy migration (EM) into the $^3H_4$ level ($^3H_4,^3H_6 \rightarrow ^3H_6,^3H_4$) are also indicated. In Fig. 2 is represented the 1/*e* time of the $^3H_4$ Tm^{3+} level as a function of concentration. Such time constant is defined as $\Phi(\tau_{1/e})=\Phi(0)/e$, where $\Phi(t)$ is the luminescent signal and $\Phi(0)$ corresponds to its intensity at time zero. As the 1/*e* time varies 3 orders of magnitude with Tm^{3+} concentration, the results are presented in a log scale in order to obtain a better visualization. As Tm^{3+} concentration increases, the decay curves become faster and nonexponential characterizing the quenching mechanism produced by the cross relaxation. The solid and dotted lines in the figure are simulations of the 1/*e* time as will be discussed later.

IV. DISCUSSIONS

A rate equations formalism was used to evaluate the effect of the energy transfer in the 1/*e* time of the $^3H_4$ level of Tm^{3+}. Based on the energy levels of Fig. 1(a), the following rate equations can be written:

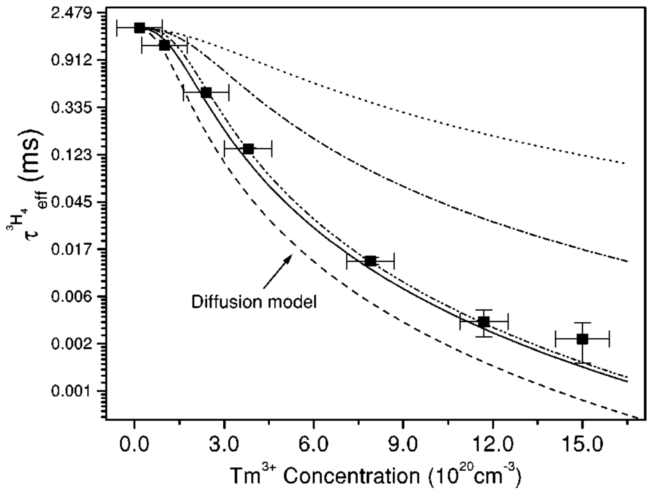

FIG. 2. 1/*e* time of the $^3H_4$ level in function of Tm concentration (solid squares) and simulations of the effective $^3H_4$ level lifetime with all the multipole couplings in the hopping model (solid line). The dotted, dash-dotted, and dash-dotted-dotted lines are simulations and with only dipole-dipole, dipole-quadrupole, and quadrupole-quadrupole couplings, respectively, in the hopping model. The dashed line is a simulation with all the multipole couplings in the diffusion model.

$$\frac{dn_0}{dt}=-Rn_0-W_{\mathrm{ET}}n_2n_0+n_2W_{20}+n_1W_{10},$$

$$\frac{dn_1}{dt}=2W_{\mathrm{ET}}n_2n_0+n_2W_{21}-n_1W_{10}, \qquad (1)$$

$$\frac{dn_2}{dt}=Rn_0-W_{\mathrm{ET}}n_2n_0-n_2W_{20}-n_2W_{21},$$

where n_0, n_1, and n_2 are the $^3H_6$, $^3F_4$, and $^3H_4$ levels, respectively. W_{ij} is the transition rate from level *i* to level *j*, W_{ET} is the energy transfer parameter given in cm^3/s and $R=\sigma I/h\nu$ is the pumping rate, where σ is the absorption cross section at the pumping energy ($h\nu$) and *I* is the intensity of the pump light. These coupled rate equations can be easily solved considering a low excitation density, in this case n_0 is constant and can be approximated by the total concentration n_t. In this case, we have for the n_2 level ($^3H_4$) the following equation:

$$\frac{dn_2}{dt}=Rn_t-n_2\left(\frac{1}{\tau_0^{n_2}}+W_{\mathrm{ET}}n_t\right)=Rn_t-\frac{n_2}{\tau_{\mathrm{eff}}^{n_2}}, \qquad (2)$$

where $(\tau_0^{n_2})^{-1}=W_{21}+W_{20}=70s^{-1}+470s^{-1}$ is the inverse of the $^3H_4$ lifetime in the absence of energy transfer (low concentrated sample) and $\tau_{\mathrm{eff}}^{n_2}$ is called the effective lifetime of the $^3H_4$ and is given by

$$(\tau_{\mathrm{eff}}^{n_2})^{-1}=\frac{1+W_{\mathrm{ET}}n_t\tau_0^{n_2}}{\tau_0^{n_2}}. \qquad (3)$$

The expressions for $n_2(t)$ and $n_2(\infty)$ are obtained by integrating Eq. (2) for a pump pulse and a steady state pumping, respectively, with the results

$$n_2(t)=n_2(0)e^{-t/\tau_{\mathrm{eff}}^{n_2}} \text{ and } n_2(\infty)=Rn_t\tau_{\mathrm{eff}}^{n_2}. \tag{4}$$

It is worth noting that the above rate equations treatment is an approximation and the obtained decay constants represent an average of the $1/e$ decay. The effective lifetime is a function of the Tm^{3+} concentration (n_t) and of the energy transfer parameter (W_{ET}), which can be calculated on the basis of the microscopic parameters of energy transfer.[24,25,27] The expression for W_{ET} will depend on the energy migration regime (diffusion limited energy transfer[28] or hopping model[25]) and on the multipole order of the interaction. Following the same procedure outlined in Ref. 29 for the dipole-dipole energy transfer rate (W_{ET}^{dd}) in the hopping and diffusion models, the W_{ET}^{dq} and W_{ET}^{qq} parameters can also be obtained. This is done by using the Inokuti-Hirayama[30] and Martin[31] expressions for the donor decay curve in the static and diffusion assisted regimes, respectively.

In the hopping model, the excitation energy jumps among the donors until a donor-acceptor interaction or a nonradiative decay occurs. In this case, the donor luminescence is described by

$$\Phi(t)=\rho^{(s)}(t)e^{-t/\tau_j}+\frac{1}{\tau_j}\int_0^t\Phi(t-t')\rho^{(s)}(t')e^{-t'/\tau_j}dt', \tag{5}$$

where s indicates the multipole order of interaction and can be 6, 8, or 10 for dipole-dipole, dipole-quadrupole, or quadrupole-quadrupole, respectively, τ_j is the jump time and $\rho^{(s)}(t)=\exp[-t/\tau_0-n_d(4\pi/3)\Gamma(1-3/s)(C_{d\text{-}d}^{(s)}t)^{3/s}]$ $=\exp[-t/\tau_0-(A^{(s)})^{3/s}t^{3/s}]$, n_d is the donor concentration, and $C_{d\text{-}d}^{(s)}$ is the microparameter of energy transfer between the donors that depends on the multipole order. This function can be written as

$$\rho^{(s)}(t)=\int_0^\infty e^{-Wt}\Phi(W)dW, \tag{6}$$

where $\Phi(W)dW=(A/4\pi)^{1/2}W^{-3/2}e^{-A/4W}dW$ is a normalized function which gives the probability that the transfer rate will be between W and $W+dW$. The jump time τ_j $=A/6$ is given by the maximum of $\Phi(W)$. A critical radius R_c where the donor-acceptor interaction is equal to the donor-donor interaction can be defined such as $P_{d\text{-}a}^{(s)}=R_0^s/\tau_0$ $=R_c^s/\tau_j$, where R_0 is the critical distance at which the donor-acceptor interaction is equal to the spontaneous decay rate ($1/\tau_0$). The energy transfer rate is equal to the number of acceptors that falls into this strong interaction sphere per unit time:

$$P^{(s)}=\frac{4\pi}{3}R_c^3n_a\frac{1}{\tau_0}=W_{\mathrm{ET}}^{(s)}n_a, \tag{7}$$

where n_a is the acceptor concentration.

TABLE I. $W_{\mathrm{ET}}^{(s)}$ parameters obtained for the diffusion limited and hopping model, n_d is the donor concentration.

	Diffusion model	Hopping model
W_{ET}^{dd}	$28(C_{d\text{-}a}^{dd})^{1/4}(C_{d\text{-}d}^{dd})^{3/4}n_d$	$13(C_{d\text{-}a}^{dd})^{1/2}(C_{d\text{-}d}^{dd})^{1/2}n_d$
W_{ET}^{dq}	$31(C_{d\text{-}a}^{dq})^{1/6}(C_{d\text{-}d}^{dq})^{5/6}n_d^{5/3}$	$21(C_{d\text{-}a}^{dq})^{3/8}(C_{d\text{-}d}^{dq})^{5/8}n_d^{5/3}$
W_{ET}^{qq}	$57(C_{d\text{-}a}^{qq})^{1/8}(C_{d\text{-}d}^{qq})^{7/8}n_d^{7/3}$	$42(C_{d\text{-}a}^{qq})^{3/10}(C_{d\text{-}d}^{qq})^{7/10}n_d^{7/3}$

In the diffusion limited regime, the expression for the energy transfer rate is obtained by making $x\to\infty$ in the expression for the donor decay[31]

$$\Phi(t)=\Phi(0)\exp\left[-\frac{t}{\tau_0}-\frac{4\pi}{3}n_a\Gamma\left(1-\frac{3}{s}\right)\times(C_{d\text{-}a}^{(s)}t)^{3/s}\left(\frac{1+a_1x+a_2x^2}{1+b_1x}\right)^{(s-3)/(s-2)}\right], \tag{8}$$

where $x=D^{(s)}(C_{d\text{-}a}^{(s)})^{-2/s}t^{1-2/s}$, the values of the constants a_1, a_2, and b_1 depend on the multipole order of the interaction[31] and the diffusion constant is given by $D^{(s)}$ $=[1/(2s-10)](4\pi/3)^{[s-2]/3}n_d^{[s-5]/3}C_{d\text{-}d}^{(s)}$. In this case, we have that

$$\Phi(t)=\Phi(0)\exp\left[-\frac{t}{\tau_0}-\frac{4\pi}{3}n_a\Gamma\left(1-\frac{3}{s}\right)\times(C_{d\text{-}a}^{(s)}t)^{3/s}\left(\frac{a_2x}{b_1}\right)^{(s-3)/(s-2)}\right]. \tag{9}$$

The above equation can be simplified to take the form

$$\Phi(t)=\Phi(0)\exp\left[-\frac{t}{\tau_0}-W_{\mathrm{ET}}^{(s)}n_at\right]. \tag{10}$$

Table I lists the expressions for $W_{\mathrm{ET}}^{(s)}$ in the two models. It

TABLE II. Microparameters of energy transfer obtained by Dexter (dipole-dipole) and Kushida (dipole-quadrupole and quadrupole-quadrupole) models for the donor-acceptor ($^3\mathrm{H}_4,{}^3\mathrm{H}_6\to{}^3\mathrm{F}_4,{}^3\mathrm{F}_4$) and donor-donor ($^3\mathrm{H}_4,{}^3\mathrm{H}_6\to{}^3\mathrm{H}_6,{}^3\mathrm{H}_4$) interactions as obtained in Ref. 17. The errors could be included in the dipole-dipole and dipole-quadrupole terms because the real concentrations were measured by EDX in this work. The calculation of the quadrupole-quadrupole term does not depend on concentration and its error could not be estimated.

$C_{d\text{-}a}^{dd}$(cm^6/s)	$C_{d\text{-}d}^{dd}$(cm^6/s)	$C_{d\text{-}a}^{dq}$(cm^8/s)	$C_{d\text{-}d}^{dq}$(cm^8/s)	$C_{d\text{-}a}^{qq}$(cm^{10}/s)	$C_{d\text{-}d}^{qq}$(cm^{10}/s)
$(2\pm0.2)\times10^{-40}$	$(6\pm1)\times10^{-40}$	$(5.5\pm0.5)\times10^{-54}$	$(22\pm2)\times10^{-54}$	12×10^{-68}	87×10^{-68}

TABLE III. Macroscopic parameters of energy transfer obtained by replacing the microparameters listed Table II into the expressions of Table I for the hopping and diffusion models. n_{Tm} is the Tm^{3+} concentration.

	W_{ET}^{dd}	W_{ET}^{dq}	W_{ET}^{qq}
Hopping model	$(3.8\text{-}5.0)\times10^{-39}$ $\mathrm{cm}^6\,\mathrm{s}^{-1} n_{Tm}$	$(2.5\text{-}3.0)\times10^{-52}$ $\mathrm{cm}^8\,\mathrm{s}^{-1} n_{Tm}^{5/3}$	2×10^{-65} $\mathrm{cm}^{10}\,\mathrm{s}^{-1} n_{\mathrm{Tm}}^{7/3}$
Diffusion model	$(11\text{-}15)\times10^{-39}\mathrm{cm}^6\,\mathrm{s}^{-1} n_{Tm}$	$(5.0\text{-}6.0)\times10^{-52}$ $\mathrm{cm}^8\,\mathrm{s}^{-1} n_{Tm}^{5/3}$	4×10^{-65} $\mathrm{cm}^{10}\,\mathrm{s}^{-1} n_{\mathrm{Tm}}^{7/3}$

must be noted that the concentration dependence is always stronger in the high-order mechanisms.

In a recent paper[17] the energy transfer microparameters for the cross relaxation and the energy migration represented in Fig. 1 were calculated by Dexter[18] and Kushida[19] models. It was shown that even though the Martin[31] expression for dipole-quadrupole interaction could fit the decay curves of the $^3\mathrm{H}_4$ level (Fig. 4 of Ref. 17), the adjusted expression did not yield meaningful values for the energy transfer microparameters $C_{d\text{-}a}^{dq}$ and $C_{d\text{-}d}^{dq}$ because they were not found to be constant as concentration changed. The conclusion was that the Tm:Tm interactions in fluoroindogallate glass should be described by a combination of all the multipole couplings and also that the diffusion limited regime is not valid in the system. The microscopic parameters of energy transfer for the CR and EM processes were calculated and are listed in Table II, as the $C_{d\text{-}d}^{(s)}$ microparameters are larger than the $C_{d\text{-}a}^{(s)}$ the condition for applying the hopping model is fulfilled.[25]

In this sense, the W_{ET} parameter in Eqs. (1) must be a sum over all the energy transfer interactions in the Hopping model $W_{\mathrm{ET}} = W_{\mathrm{ET}}^{dd} + W_{\mathrm{ET}}^{dq} + W_{\mathrm{ET}}^{qq}$. The calculated $W_{\mathrm{ET}}^{(s)}$ parameters are listed in Table III and were used to simulate $\tau_{\mathrm{eff}}^{n_2}$ [Eq. (4)]. Such simulation is represented as a solid line in Fig. 2 and was carried out using the mean values of $W_{\mathrm{ET}}^{(s)}$ $W_{\mathrm{ET}} = 4.4\times10^{-39} n_{Tm}$ $\mathrm{cm}^6\,\mathrm{s}^{-1} + 2.8\times10^{-52} n_{Tm}^{5/3}$ $\mathrm{cm}^8\,\mathrm{s}^{-1} + 2.0\times10^{-65} n_{Tm}^{7/3}$ $\mathrm{cm}^{10}\,\mathrm{s}^{-1}$. The good agreement between the calculated $\tau_{\mathrm{eff}}^{n_2}$ and the experimental $1/e$ time corroborates our previous assumption that the high-order interactions dominate the Tm:Tm energy transfer. It was verified that the simulated curve is not so much sensitive to the W_{ET}^{dd} and W_{ET}^{dq} parameters, but it is strongly dependent on W_{ET}^{qq}. The dotted, dash-dotted, and dash-dotted-dotted lines are simulations considering only dipole-dipole, dipole-quadrupole, and quadrupole-quadrupole interactions, respectively. It can be noted that the quadrupole-quadrupole mechanism best describes the $1/e$ time of the $^3\mathrm{H}_4$ level which means that it is the most important mechanism of energy transfer. The dashed line in Fig. 2 represents the simulation of the $^3\mathrm{H}_4$ effective lifetime using all the multipole coupling mechanisms and the W_{ET} parameter obtained via the diffusion model. It can be seen that the agreement is lost in this situation as an evidence of the inadequacy of the diffusion model to describe the system.

Table IV shows a comparison among the microparameters found in Refs. 13 and 16 and in Ref. 17 for the $\mathrm{Tm}^{3+}:\mathrm{Tm}^{3+}$ interactions in the infrared region. In these works, Dexter[18] and Kushida[19] models were used to calculate the energy transfer microparameters. As the energy transfer microparameters depend on the overlap integral and on the intensities of the absorption and emission cross sections of the involved electronic transitions, one can try to correlate the microparameters found in the two hosts with the aspect of inhomogeneous broadening that is stronger in glasses than in crystals. For example, the $\mathrm{C}_{d\text{-}a}^{dd}$ is higher in the glass than in the YLF crystal and this can be due to the broadening of the band profiles in glasses that provides a larger spectral overlap if the energy transfer is nonresonant, as is the case. On the other hand, the $\mathrm{C}_{d\text{-}d}^{dd}$ is lower in the glass, which denotes the compromise between overlap and intensity of the involved bands. In case of a resonant process the intensity is crucial for a high-energy transfer parameter. The $\mathrm{C}_{d\text{-}a}^{dq}$ and $\mathrm{C}_{d\text{-}a}^{qq}$ microparameters are greater in the YLF crystal than in the fluoroindogallate glass, this can be due to a higher intensity of the quadrupole transition in the crystal. Armagan *et al.*[7] have applied the Dexter model to calculate the $^3\mathrm{H}_4,{}^3\mathrm{H}_6 \rightarrow {}^3\mathrm{F}_4,{}^3\mathrm{F}_4$ cross-relaxation microparameter in Tm^{3+} doped yttrium aluminum garnet (YAG) crystal. The energy transfer microparameter was found to be $\mathrm{C}_{d\text{-}a}^{dd} = 27\times10^{-40}$ cm^6/s, which is larger than the corresponding values obtained for the YLF and fluoroindogallate glass. Such difference can be attributed to the larger phonon energy of the YAG crystal as compared to YLF and fluoroindogallate glass which favors the nonresonant $^3\mathrm{H}_4,{}^3\mathrm{H}_6 \rightarrow {}^3\mathrm{F}_4,{}^3\mathrm{F}_4$ energy transfer.

Xueyuan and Zundu[26] calculated the $\mathrm{C}_{d\text{-}a}^{dd}$ microparameter for the same cross-relaxation in Tm^{3+} doped yttrium orthovanadate crystal (YVO_4) by means of Dexter model and found $\mathrm{C}_{d\text{-}a}^{dd} \approx 10\times10^{-40}$ cm^6/s. On the other hand, Bettinelli[6] and co-workers used the Inokuti-Hirayama expression in the dipole-dipole approximation to fit the decay

TABLE IV. Comparison between the energy transfer microparameters found in YLF crystal with the ones obtained in the Fluoroindogallate glass (FG).

	$\mathrm{C}_{d\text{-}a}^{dd}$ $\times10^{40}$ cm^6/s	$\mathrm{C}_{d\text{-}d}^{dd}$ $\times10^{40}$ cm^6/s	$\mathrm{C}_{d\text{-}a}^{dq+qd}$ $\times10^{54}$ cm^8/s	$\mathrm{C}_{d\text{-}d}^{dq+qd}$ $\times10^{54}$ cm^8/s	$\mathrm{C}_{d\text{-}a}^{qq}$ $\times10^{68}$ $\mathrm{cm}^{10}/\mathrm{s}$	$\mathrm{C}_{d\text{-}d}^{qq}$ $\times10^{68}$ $\mathrm{cm}^{10}/\mathrm{s}$	Refs.
YLF	0.94	17.3	9.4	66.5	42	476	13,16
FG	2.0	6.0	6.4	24	12	87	17

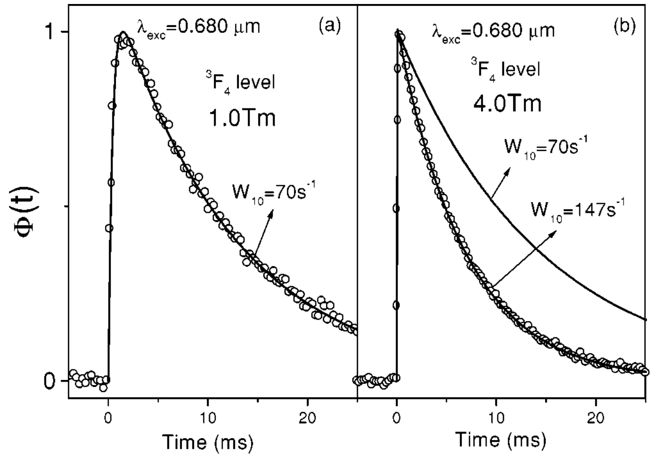

FIG. 3. Temporal behavior of the $^3F_4$ level luminescence for the (a) 1 Tm and (b) 4 Tm samples (open circles). The solid lines are the solutions of Eq. (11) using the W_{ET} obtained for the hopping model. The used value for W_{10} in the simulations is indicated in each curve.

curves of the $^3H_4$ level of Tm^{3+} in YVO_4. Such procedure leads to $C_{d\text{-}a}^{dd} = 18\times10^{-40}$ cm^6/s in a clear demonstration of the overestimation of the cross-relaxation parameter when using the dipole-dipole interaction to fit the decay curves. Martin[32] and Li[33] have applied the Yokota-Tanimoto (YT)[28] model to fit the decay curves of the $^3H_4$ level of Tm^{3+} in an indium based fluoride glass and a Y_2SiO_5 crystal, respectively. These two works obtained $C_{d\text{-}a}^{dd} = 13\times10^{-40}$ cm^6/s, $C_{d\text{-}d}^{dd} = 3\times10^{-40}$ cm^6/s,[32] $C_{d\text{-}a}^{dd} = 60\times10^{-40}$ cm^6/s and $C_{d\text{-}d}^{dd} = 7\times10^{-40}$ cm^6/s.[33] This same feature ($C_{d\text{-}a}^{dd} > C_{d\text{-}d}^{dd}$) was observed in Ref. 17 when applying the YT model to the $^3H_4$ level decay curves in fluoroindogallate glass. Such result is not expected as the cross relaxation $^3H_4, {}^3H_6 \rightarrow {}^3F_4, {}^3F_4$ is nonresonant and, consequently, the spectral overlap is larger for the energy migration $^3H_4, {}^3H_6 \rightarrow {}^3H_6, {}^3H_4$.

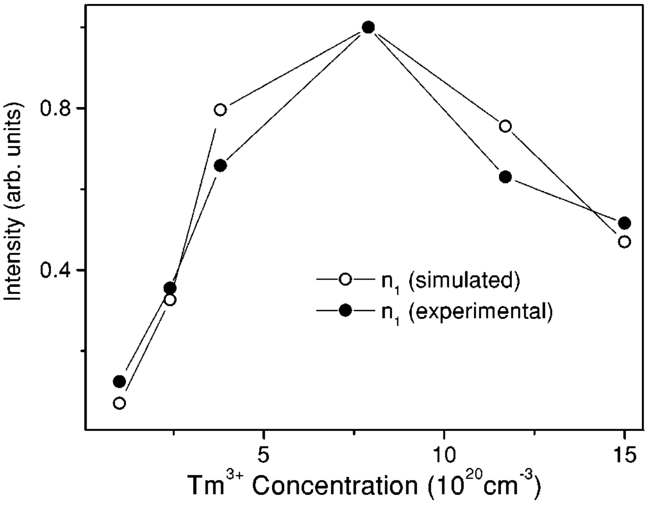

FIG. 4. Integrated intensity of the $^3F_4 \rightarrow {}^3H_6$ (solid circles) electronic transition in function of Tm^{3+} concentration. The open circles represent the simulated steady state population of the $^3F_4$ level obtained in the hopping model. The lines are guides to the eye.

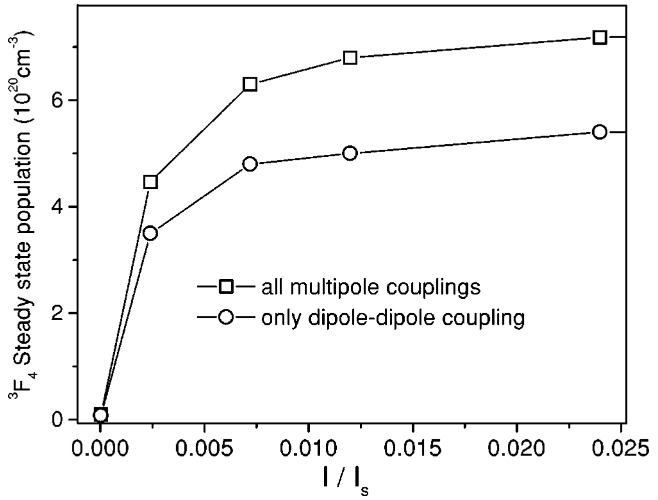

FIG. 5. Steady state population of the $^3F_4$ level obtained by the solution of the rate equations (1) with all the multipole couplings (open squares) and with only the dipole-dipole coupling (open circles) in the hopping model.

Concerning the $^3F_4$ level, the solution of the rate equations for $n_1(t)$ is given by

$$n_1(t) = \frac{n_2(0)(2W_{\mathrm{ET}}n_t + W_{21})}{W_{10} - (\tau_{\mathrm{eff}}^{n_2})^{-1}} (e^{-t/\tau_{\mathrm{eff}}^{n_2}} - e^{-W_{10}t}), \quad (11)$$

where $W_{10} = 83$ s^{-1} and $W_{21} = 70$ s^{-1} are, respectively, the $^3F_4 \rightarrow {}^3H_6$ and $^3H_4 \rightarrow {}^3H_6$ decay rates that were obtained by Judd-Ofelt calculations. Figures 3(a) and 3(b) show the time evolution of the $^3F_4$ level population (open circles) and the simulations (solid lines) obtained with Eq. (11). All samples presented an exponential decay time after a faster risetime as the Tm^{3+} concentration increases. It can be noted that the decay curve of the high concentrated sample is faster than the low concentrated one, which is not predicted by Eq. (11). Such a result characterizes an energy migration within the $^3F_4$ level with a subsequent energy transfer to a lattice defect causing a reduction of the $^3F_4$ lifetime. Another possibility is an upconversion mechanism in which two Tm ions in the $^3F_4$ level interact in such way that one of them goes to the ground state and the other is excited to the $^3H_4$ level. The best fitted solid line in Fig. 3(b) was obtained by the inclusion of the experimental lifetime of the $^3F_4$ level ($\tau_{\mathrm{exp}}^{n_1}$) in Eq. (11).

The steady state population of the $^3F_4$ level is also affected by the quenching mechanism as can be seen at the intensity of the $^3F_4 \rightarrow {}^3H_6$ transition in function of Tm^{3+} concentration. In the absence of quenching, the steady state population of the $^3F_4$ level $[n_1(\infty)]$ can be calculated by doing $dn_1/dt = 0$, which gives the result

$$n_1(\infty) = \frac{n_2(\infty)(2W_{\mathrm{ET}}n_t + W_{21})}{W_{10}}, \quad (12)$$

where $n_2(\infty) = Rn_t\tau_{\mathrm{eff}}^{n_2}$ is the steady state population of the $^3H_4$ level. Substituting $n_2(\infty)$ into Eq. (12), we have

$$n_1(\infty)=\frac{R n_t(2W_{\mathrm{ET}}n_t+W_{21})\tau_0^{n_2}}{W_{10}(1+W_{\mathrm{ET}}n_t\tau_0^{n_2})}. \tag{13}$$

A plot of $n_1(\infty)$ as a function of Tm^{3+} concentration would lead to a linear relation between these two quantities which is not experimentally observed. The solid circles in Fig. 4 represent the integrated intensity of $^3F_4 \rightarrow {}^3H_6$ electronic transition in function of Tm^{3+} concentration. The open circles are simulations of the steady state population of the $^3F_4$ level with W_{10} equal to $(\tau_{\mathrm{exp}}^{n_1})^{-1}$. The low signal gain of the $^3F_4 \rightarrow {}^3H_6$ transition will follow the same trends as in Fig. 4, but as the pump density increases Eq. (13) does not represent the steady state population anymore and the optimum concentration changes to high values.

Figure 5 shows the calculated population of the $^3F_4$ level for the 4Tm sample obtained by the numerical solution of the rate equations in two cases: only the dipole-dipole interaction ($W_{\mathrm{ET}}=3.2\times10^{-18}$ cm^3/s) and with all the multipole orders included ($W_{\mathrm{ET}}=1.4\times10^{-16}$ cm^3/s). The W_{ij} parameters were $W_{21}=70$ s^{-1}, $W_{20}=470$ s^{-1}, and $W_{10}=(\tau_{\mathrm{exp}}^{n_1})^{-1}=147$ s^{-1}. It can be noted that the underestimation of the $^3F_4$ population is about 22% for pump densities above 0.01 of the saturation intensity and could lead to significant errors in the estimation of some laser parameters such as the gain factor. It is also important to see the high density of excited ions accumulated in the $^3F_4$ level due to its long lifetime.

V. CONCLUSIONS

The Tm:Tm energy transfer in fluoroindogallate glasses was analyzed by means of rate equations and microscopic parameters of energy transfer. The effective lifetime of the $^3H_4$ level was successfully described by the inclusion of the dipole-quadrupole and quadrupole-quadrupole coupling mechanisms in the Tm:Tm energy transfer processes $^3H_4, {}^3H_6 \rightarrow {}^3F_4, {}^3F_4$ and $^3H_4, {}^3H_6 \rightarrow {}^3H_6, {}^3H_4$. The results obtained in this work are in good agreement with the previous observations reported in Ref. 17 which showed that the mentioned energy transfer processes between Tm ions in fluoroindogallate glasses is dominated by the dipole-quadrupole and quadrupole-quadrupole coupling mechanisms. It is important to note that if the high-order interactions are neglected in the Tm^{3+}:Tm^{3+} energy transfer, the $^3F_4$ steady state population, which is an important parameter for the laser system, will be underestimated.

ACKNOWLEDGMENTS

The authors wish to thank Dr. N. J. H. Gallo for the EDX measurements. This work was supported by Conselho Nacional de Desenvolvimento Científico e Tecnológico (CNPq), Fundação de Amparo à Pesquisa do Estado de São Paulo (FAPESP), and FINEP.

---

[1] E. Rukmini and C. K. Jayasankar, J. Non-Cryst. Solids **176**, 213 (1994), and references there in.

[2] R. Kaufmann, A. Hartmann, R. Hibst, and J. Dermat, Surg. Oncol. **20**, 112 (1994).

[3] G. R. Osche and D. s. Young, Proc. IEEE **84**, 103 (1996).

[4] W. Ryba-Romanowski, M. Berkowski, B. Viana, and P. Aschehoug, Appl. Phys. B: Lasers Opt. **64**, 525 (1997).

[5] W. Ryba-Romanowski, S. Golab, G. Dominiak-Dzik, M. Zelechower, and J. Gabrys-Pisarska, J. Alloys Compd. **325**, 215 (2001).

[6] M. Bettinelli, F. S. Ermeneux, R. Moncorgé, and E. Cavalli, J. Phys.: Condens. Matter **10**, 8207 (1998).

[7] G. Armagan, A. M. Buoncristiani, and B. DiBartolo, Opt. Mater. **1**, 11 (1992).

[8] A. Brenier, C. Madej, C. Pedrini, and G. Boulon, J. Phys.: Condens. Matter **3**, 203 (1991).

[9] L. G. V. Uitert and L. F. Johnson, J. Chem. Phys. **44**, 3514 (1965).

[10] L. G. V. Uitert, E. F. Dearborn, and J. J. Rubin, J. Chem. Phys. **45**, 1578 (1966).

[11] L. Gomes, L. C. Courrol, L. V. G. Tarelho, and I. M. Ranieri, Phys. Rev. B **54**, 3825 (1996).

[12] E. Nakazawa and S. Shionoya, J. Chem. Phys. **47**, 3211 (1967).

[13] A. M. Tkachuk, I. K. Razumova, M. F. Joubert, R. Moncorgè, D. I. Mironov, and A. A. Nikitichev, Opt. Spektrosk. **85**, 965 (1998) [Opt. Spectrosc. **85**, 885 (1998)].

[14] T. T. Basiev, Yu. V. Orlovskii, and Yu. S. Privis, J. Lumin. **69**, 187 (1996).

[15] K. Tonooka, K. Yamada, N. Kamata, and F. Maruyama, J. Lumin. **60&61**, 864 (1994).

[16] A. M. Tkachuk, I. K. Razumova, E. Yu. Perlin, M. F. Joubert, and R. Moncorgè, Opt. Spektrosk. **90**, 88 (2001) [Opt. Spectrosc. **90**, 78 (2001)].

[17] D. F. de Sousa, R. Lebullenger, A. C. Hernandes, and L. A. O. Nunes, Phys. Rev. B **65**, 094204 (2002).

[18] D. L. Dexter, J. Chem. Phys. **21**, 836 (1953).

[19] T. Kushida, J. Phys. Soc. Jpn. **34**, 1318 (1973).

[20] V. Ostroumov, T. Jensen, J. P. Meyn, G. Huber, and M. A. Noginov, J. Opt. Soc. Am. B **15**, 1052 (1998).

[21] J. L. Doualan, C. Maunier, D. Descamps, J. Landais, and R. Moncorgè, Phys. Rev. B **62**, 4459 (2000).

[22] S. Guy, C. L. Bonner, D. P. Shepherd, D. C. Hanna, A. C. Troper, and B. Ferrand, IEEE J. Quantum Electron. **34**, 900 (1998).

[23] S. A. Payne, L. K. Smith, R. J. Beach, B. H. T. Chai, J. H. Tassano, L. D. DeLoach, W. L. Kway, R. W. Solarz, and W. F. Krupke, Appl. Opt. **33**, 5526 (1994).

[24] Yu K. Voronko, T. G. Mamedov, V. V. Osiko, A. M. Prokhorov, V. P. Sakun, and A. I. Scherbakov, Sov. Phys. JETP **44**, 251 (1976).

[25] A. I. Burshtein, Sov. Phys. JETP **35**, 882 (1972).

[26] C. Xueyuan and Luo Zundu, J. Phys.: Condens. Matter **9**, 7981 (1997).

[27] S. A. Payne, G. D. Wilke, L. K. Smith, and W. F. Krupke, Opt. Commun. **111**, 263 (1994).

[28] M. Yokota and F. Tanimoto, J. Phys. Soc. Jpn. **22**, 779 (1967).

[29] Baldassare Di Bartolo, in *Energy Transfer Processes in Condensed Matter*, *NATO Advanced Studies Institute* (Plenum Press, New York, 1983), p. 156.

[30] M. Inokuti and F. Hirayama, J. Chem. Phys. **43**, 1978 (1965).

[31] I. R. Martin, V. D. Rodriguez, U. R. Rodriguez-Mendoza, V. Lavin, E. Montoya, and D. Jaque, J. Chem. Phys. **111**, 1191 (1999).

[32] I. R. Martin, V. D. Rodriguez, R. Acalá, and R. Cases, J. Non-Cryst. Solids **161**, 294 (1993).

[33] C. Li, A. Lagriffoul, R. Moncorge, J. C. Souriau, C. Borel, and Ch. Wyon, J. Lumin. **62**, 157 (1994).